Journal of the Ceramic Society of Japan 121 [7] 568-571 2013 Technical report

Microstructure and mechanical properties of MgO-doped Al_2TiO_5 prepared by reactive sintering

Ryosuke MAKI[*] and Yoshikazu SUZUKI[*,,†]**

[*]Graduate School of Pure and Applied Sciences, University of Tsukuba, 1–1–1 Tennodai, Ibaraki 305–8573, Japan
[**]Faculty of Pure and Applied Sciences, University of Tsukuba, 1–1–1 Tennodai, Ibaraki 305–8573, Japan

MgO-doped Al_2TiO_5 ceramics were reactively sintered from commercial α-Al_2O_3, TiO_2 anatase and $MgCO_3$ (basic) powders. Powder mixtures with molar ratio of Al_2O_3:TiO_2:MgO = 1:1:0, 1:0.95:0.05, 1:0.90:0.10, and 1:0.85:0.15 were prepared by wet ball-milling with ZrO_2 media. The green pellets were sintered at 1300–1500°C for 2 h in air to obtain dense samples. With changing the MgO doping amount, Al_2TiO_5/Al_2O_3, $Al_2TiO_5/MgAl_2O_4/Al_2O_3$, $Al_2TiO_5/MgAl_2O_4$ composites were synthesized. MgO doping was effective to reduce the Al_2TiO_5 matrix grain size and to reduce the strong anisotropy of Al_2TiO_5, which resulted in fewer microcracks. The maximum strength of samples sintered at 1400 and 1500°C were 106 and 32 MPa (15 mol % MgO), respectively.

Key-words : Al_2TiO_5, MgO, $MgAl_2O_4$, Fracture strength

[Received May 1, 2013; Accepted May 26, 2013]

1. Introduction

Aluminum titanate (Al_2TiO_5:AT) is widely known as a low thermal expansion material with pseudobrookite structure.[1),2)] Al_2TiO_5 has high thermal shock resistance and relatively good chemical stability, and thus it is used as ladles for molten metals and light-weight structural components at high temperatures. Recently, Al_2TiO_5 is also applied for diesel particulate filters.[3)–7)] However, due to its relatively low mechanical properties caused by microcracks,[8)–10)] commercial applications of Al_2TiO_5 are limited. These microcracks are attributed to anisotropic thermal expansion of Al_2TiO_5 under cooling from the sintering temperature. In order to solve this problem, magnesium dititanate, $MgTi_2O_5$,[11)–14)] which also has a pseudobrookite structure but less anisotropy than Al_2TiO_5, and Al_2TiO_5–$MgTi_2O_5$ solid solutions[15)–18)] have been investigated.

On the other hand, dispersion strengthening enhances mechanical properties of Al_2TiO_5-based ceramics. For example, Al_2TiO_5/mullite composite,[19),20)] Al_2TiO_5/Mg_2SiO_4 composite,[21)] and $Al_2TiO_5/MgAl_2O_4$(SS)/Al_2O_3 composite[22)] have been synthesized and their mechanical properties have been reported. As Ohya et al.[22)] reported, $MgAl_2O_4$ spinel phase can be dispersed in Al_2TiO_5 as a secondary phase by controlling the ratio of Al_2O_3, TiO_2 and MgO. However, the effects of the MgO contents were not studied in detail.

In this study, we have reactively sintered MgO-doped Al_2TiO_5 ceramics from α-Al_2O_3, TiO_2 anatase and $MgCO_3$ (basic) powders, with changing the MgO doping amount to form $MgAl_2O_4$ as a secondary phase. For characterization, X-ray diffraction, microstructure and fracture strength of MgO-doped Al_2TiO_5 were investigated. In addition, the relationship between MgO amount and mechanical strength was also discussed.

2. Experimental

2.1 Sample preparation

Commercial α-Al_2O_3 (99.99% purity, Taimei Chemicals Co. Ltd., Saitama, Japan), TiO_2 anatase (99% purity, Kojundo Chemical Laboratory Co. Ltd.), and $MgCO_3$ (basic) [99.9% purity, Kojundo Chemical Laboratory Co. Ltd., actually composition of $Mg_5(CO_3)_4(OH)_2{\cdot}4H_2O$] powders were used as starting materials. Prior to the powder mixing, each starting powder was characterized by TG–DTA to analyze the weight-loss during the heating up to 1000°C, and required powder weight was corrected using the TG–DTA results.[23)] Powder mixtures of α-Al_2O_3, TiO_2 anatase, and $MgCO_3$ (basic) with corrected molar ratio of Al_2O_3:TiO_2:MgO = 1:1:0, 1:0.95:0.05, 1:0.90:0.10, and 1:0.85:0.15 were prepared by wet ball-milling with ZrO_2 media for 2 h using ethanol, and then the slurries were dried in an evaporator. After that, the mixed powders were dried at 80°C in air, and ball-milled with ZrO_2 media for 2 h. Finally mixed powders were sieved through a 150-mesh screen.

The mixed powders were formed into pellets (diameter of 15 mm) and into rectangular bars (4 × 6 × 50 mm) by uniaxial pressing. After that, the green samples were prepared by cold isostatic pressing (CIP) at 200 MPa for 10 min. Subsequently, the green pellets were sintered at 1300–1500°C for 2 h in air to obtain dense samples.

2.2 Characterization

Microstructure and constituent phases of sintered un-doped and MgO-doped samples were analyzed by scanning electron microscopy (TM3000 Table Microscope, Hitachi, Japan), and X-ray powder diffraction (Multiflex, Cu-K_α, 40 kV and 40 mA, Rigaku, Japan), respectively. Prior to the powder XRD measurement, sintered samples were pulverized, and the XRD patterns were collected in the range of 2θ = 10–70°. The samples were coated with Au by sputtering method (SC-701, 3.5 mA for 5 min Sanyu Electron, Japan) to observe surface of sintered samples.

In order to evaluate fracture strength, sintered rectangular bars were machined into the test pieces with dimension of ~3 × 4 × 40 mm (JIS R1601). The tensile face and corners of each sample were polished and chamfered by waterproof abrasive paper (P800, Riken Corundum Co. Ltd. Japan). Fracture strength was measured by three-point bending test with a span of 30 mm and crosshead speed of 0.5 mm min^{-1} by using a universal testing

† Corresponding author: Y. Suzuki; E-mail: suzuki@ims.tsukuba.ac.jp

DOI http://dx.doi.org/10.2109/jcersj2.121.568

machine (Autograph AG-20kNIT, Shimadzu Co. Ltd., Japan). Three to five samples were used for each measurement.

3. Results and discussion

3.1 XRD analysis

Figure 1 shows XRD patterns of the samples with changing the MgO amount, obtained by reactive sintering at (a) 1300°C, (b) 1400°C and (c) 1500°C for 2 h, respectively. At 1300°C [Fig. 1(a)], un-doped sample contained unreacted Al_2O_3 and TiO_2 as well as trace amount of Al_2TiO_5. Sample with 5 mol % MgO was composed of Al_2TiO_5 and Al_2O_3, and samples with 10–15 mol % MgO were composed of Al_2TiO_5, $MgAl_2O_4$ and Al_2O_3. The phase relation in this study was in good agreement with the previous report by Ohya.[22] The $MgAl_2O_4$ peaks became stronger with increasing MgO content from 10 to 15 mol %. As can be seen in Fig. 1(a), the Al_2TiO_5 peak at 62 to 64° shifted toward lower 2θ values as the MgO amounts were increased. The peak shift implies the formation of Al_2TiO_5 solid solution (SS) containing MgO, which resulted in lattice expansion. Due to the formation of Al_2TiO_5 (SS), Al_2TiO_5 phase was obtained at lower temperature than un-doped sample, in other words, pseudobrookite phase was stabilized by MgO doping.[2]

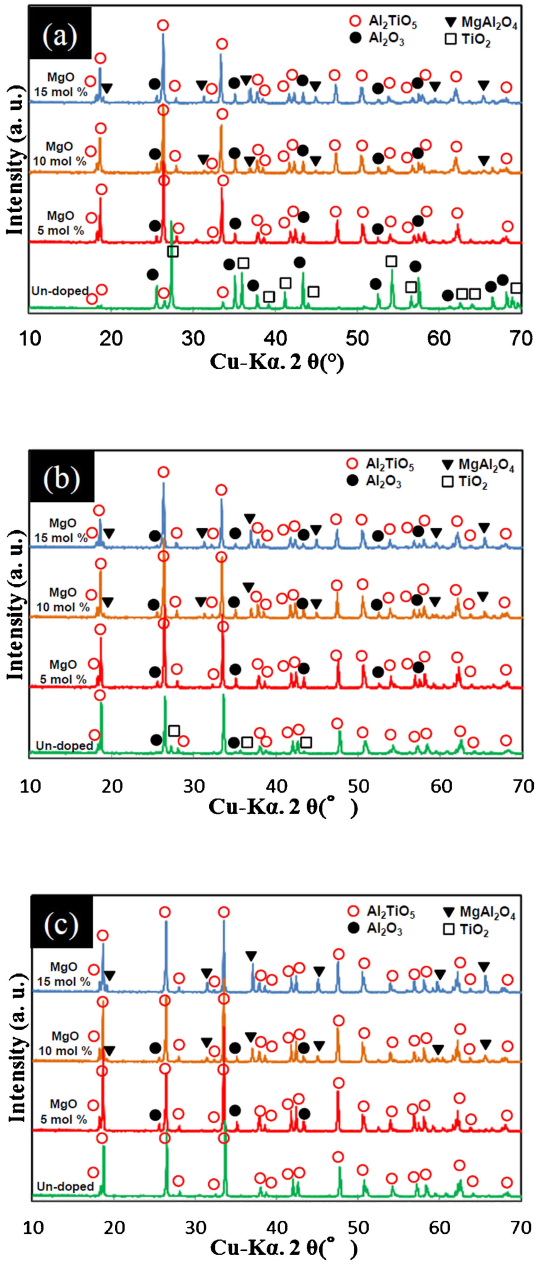

Fig. 1. XRD patterns of MgO-doped samples sintered at (a) 1300°C, (b) 1400°C and (c) 1500°C.

At 1400°C [Fig. 1(b)], even un-doped sample was composed mainly of Al_2TiO_5 with trace of Al_2O_3 and TiO_2. Samples with 5–15 mol % MgO addition sintered at 1400°C showed similar XRD patterns with those of 1300°C. Slight differences between 1300 and 1400°C samples with MgO were relatively higher crystallinity for 1400°C sample. At 1500°C [Fig. 1(c)], un-doped sample was composed of pure Al_2TiO_5 phase. Samples with 5, 10, 15 mol % MgO addition sintered at 1500°C were composed of $Al_2TiO_5 + Al_2O_3$ (5%), $Al_2TiO_5 + MgAl_2O_4 + Al_2O_3$ (10%), $Al_2TiO_5 + MgAl_2O_4$ (15%), respectively.

3.2 Microstructure

Figure 2 exhibits typical SEM images of the MgO 0–15 mol % samples sintered at 1400 and 1500°C. For samples sintered at 1400°C (upper figures), un-doped sample contained a certain amount of open pores. The matrix grains, Al_2TiO_5, were not so anisotropic. At the grain boundaries, unreacted Al_2O_3 and TiO_2 particles were observed. Sample with 5 mol % MgO consisted of relatively dense Al_2TiO_5 matrix with finer Al_2O_3 grains (~0.5–1.0 μm). Samples with 10–15 mol % MgO consisted of Al_2TiO_5 matrix with Al_2O_3 and well-faceted $MgAl_2O_4$ grains. These results were in good agreement with the XRD analysis.

For samples sintered at 1500°C (lower figures), the matrix Al_2TiO_5 grains became more anisotropic. From the SEM observation, obvious microcracks were confirmed and some liquid phase was found for un-doped, 5, and 10 mol %-MgO added samples. However, for the 15 mol %-MgO added sample, with plenty of $MgAl_2O_4$ formation, the liquid phase was almost disappeared. These results imply the formation of $MgAl_2O_4$ spinel phase occurred coincidently with the disappearance of liquid phase. The liquid phase formation can be attributed to a little contamination from Y-stabilized ZrO_2 milling media, which may produce Al_2O_3–TiO_2–MgO(–Y_2O_3)–ZrO_2 based liquid phase (confirmed by SEM-EDS, not shown). Also, a trace amount of Si-O vapor from the $MoSi_2$ heating element might decrease the liquidus temperature, because the liquid phase was found mainly on the surface of the pellets. With the sintering at 1500°C, the sample with 5 mol % MgO consisted of Al_2TiO_5 matrix with finer Al_2O_3 grains. The 10 mol % sample consisted of Al_2TiO_5 matrix with Al_2O_3 and $MgAl_2O_4$, and the 15 mol % sample consisted of Al_2TiO_5 matrix with well-faceted $MgAl_2O_4$ grains. However, for 1500°C samples, the matrix and secondary phases became larger. From the SEM observation, on the whole, the sample with MgO doping at 1400°C seemed to have higher strength due to their finer microstructure.

3.3 Mechanical property

Figure 3 demonstrates the effect of MgO amount on the fracture strength of samples sintered at 1400–1500°C. The fracture strength increased with increasing MgO amount up to 15 mol %. As is expected by SEM observation, samples with MgO doping sintered at 1400°C showed better strength. The maximum strength of samples sintered at 1400 and 1500°C were 106 and 32 MPa, respectively. The enhancement of the fracture strength can be attributed to (1) finer microstructure by the second phase dispersion and (2) fewer microcracks by the MgO doping (less anisotropic matrix grains). Table 1 shows the fracture strength of

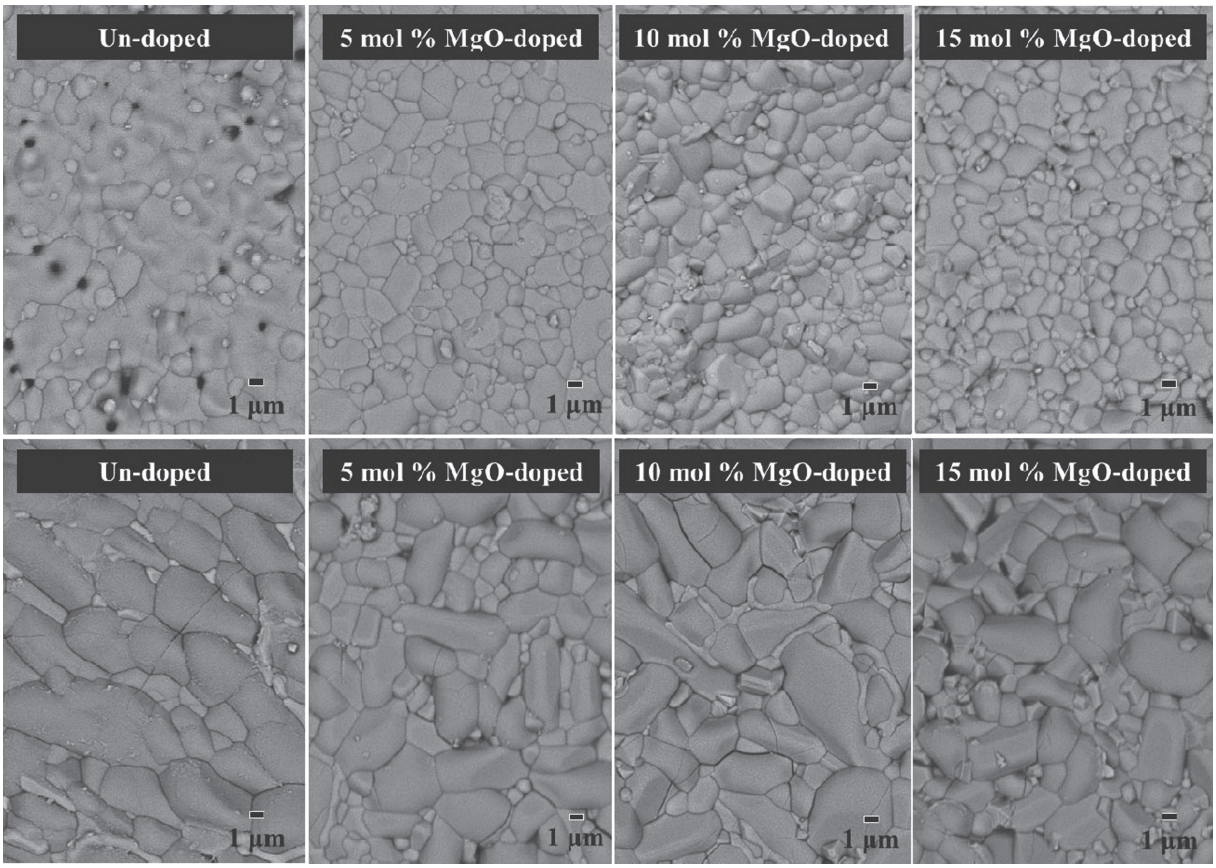

Fig. 2. SEM images of MgO-doped samples sintered at 1400°C (upper) and 1500°C (lower).

Table 1. Fracture strength of Al_2TiO_5-based ceramics

Sample	Sintering temperature (°C)	Processing characteristics	Fracture strength (MPa)	References
Al_2TiO_5(ss)/$MgAl_2O_4$	1500	Reactive sintering with Fe doping, Uniaxial press at 200 MPa	19.56	21)
Al_2TiO_5/$MgAl_2O_4$/Al_2O_3	1350	Sintering from AT powder with additives, CIP at 98 MPa	181	22)
Al_2TiO_5/Al_2O_3	1500	Sintering from Alkoxide derived AT powder	~42	24)
Al_2TiO_5/Al_2O_3	1350	Reactive sintering, Extruded sample with additives and binder	48.5	25)
Al_2TiO_5/$MgAl_2O_4$/Al_2O_3	1400	Reactive sintering, CIP at 200 MPa	106	This study

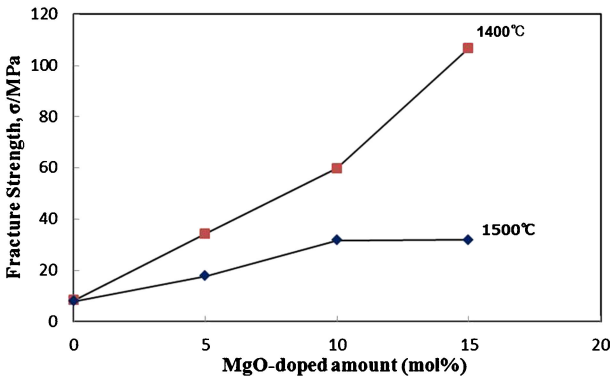

Fig. 3. Fracture strength of samples sintered at 1400 and 1500°C.

Al_2TiO_5-based ceramics in literature as well as in this study. The strength of reactively-sintered Al_2TiO_5-based ceramics in this study was not so high as that from a pre-synthesized Al_2TiO_5 powder by Ohya et al.[22] However, among the reactive sintering methods, the result in this study (106 MPa) was rather high. Thinking about the saving energy and CO_2 emission, the simplification of processing (viz., reactive sintering) will be beneficial.

4. Conclusions

In this study, MgO-doped Al_2TiO_5 ceramics were reactively sintered from α-Al_2O_3, TiO_2 anatase and $MgCO_3$ (basic) powders. The formation temperature of Al_2TiO_5 phase was decreased by MgO-doping. With changing the MgO doping amount, Al_2TiO_5/Al_2O_3, Al_2TiO_5/$MgAl_2O_4$/Al_2O_3, Al_2TiO_5/$MgAl_2O_4$ composites were synthesized. SEM observation revealed that MgO doping was effective to reduce the Al_2TiO_5 matrix grain size and to reduce the strong anisotropy of Al_2TiO_5, which resulted in fewer microcracks. The maximum strength of samples sintered at 1400 and 1500°C were 106 and 32 MPa (15 mol % MgO), respectively.

Acknowledgment The authors thank Dr. Tohru S. Suzuki for the use of SEM. We also appreciate the anonymous reviewer for the constructive comments. This work was supported by Grant-in-Aid for Science Research No. 23350111 for Basic Research: Category B.

References

1) B. Morosin and R. W. Lynch, *Acta Crystallogr., Sect. B: Struct. Crystallogr. Cryst. Chem.*, 28, 1040–1046 (1972).
2) I. J. Kim and L. G. Gauckler, *J. Ceram. Sci. Tech.*, 3, 49–60 (2012).
3) I. J. Kim, *J. Ceram. Proc. Res.*, 11, 411–418 (2010).
4) M. Backhaus-Ricoult, C. Glose, P. Tepesch, B. Wheaton and J. Zimmermann, "Advances in Bioceramics and Porous Ceramics III: Ceramic Engineering and Science Proceedings", Vol. 31, Ed. by R. Narayan, P. Colombo, S. Mathur and T. Ohji, John Wiley & Sons, Inc., Hoboken, NJ, USA. (2010) pp. 145–162.
5) S. B. Ogunwumi, P. D. Tepesch, T. Chapman, C. J. Warren, I. M. Melscoet-Chauvel and D. L. Tennent, Proceedings SAE World Congress SAE 2005-01-0583 (2005).
6) A. Nemoto, K. Iwasaki, O. Yamanishi, K. Tsuchimoto, K. Uoe, T. Toma and H. Yoshino, *Sumitomo Chem. R&D Rep.*, 2, 4–13 (2011).
7) A. Okada, *New Grass*, 21, 59–62 (2006) [in Japanese].
8) Y. Ohya and Z. Nakagawa, *J. Mater. Sci.*, 31, 1555–1559 (1996).
9) H. C. Kim, K. S. Lee, O. S. Kweon, C. G. Aneziris and I. J. Kim, *J. Eur. Ceram. Soc.*, 27, 1431–1434 (2007).
10) Q.-C. Zhang, Q.-M. Ye, G. Li, J.-H. Lin, J.-F. Song, S.-H. Chang and J. Liu, *Mater. Lett.*, 62, 832–836 (2008).
11) Y. Suzuki and M. Morimoto, *J. Ceram. Soc. Japan*, 118, 819–822 (2010).
12) Y. Suzuki and M. Morimoto, *J. Ceram. Soc. Japan*, 118, 1212–1216 (2010).
13) Y. Suzuki and Y. Shinoda, *Sci. Tech. Adv. Mater.*, 12, 034301 (2011).
14) Y. Suzuki, T. S. Suzuki, Y. Shinoda and K. Yoshida, *Adv. Eng. Mater.*, 14, 1134–1138 (2012).
15) L. Giordano, M. Viviani, C. Bottino, M. T. Buscaglia, V. Buscaglia and P. Nanni, *J. Eur. Ceram. Soc.*, 22, 1811–1822 (2002).
16) K. Daimon, *J. Ceram. Soc. Japan*, 98, 365–369 (1990).
17) V. Buscaglia, G. Battilana, M. Leoni and P. Nanni, *J. Mater. Sci.*, 31, 5009–5016 (1996).
18) T. Shimazu, M. Miura, N. Isu, T. Ogawa, K. Ota, H. Maeda and E. H. Ishida, *Mater. Sci. Eng., A*, 487, 340–346 (2008).
19) I. J. Kim and L. J. Gauckler, *J. Ceram. Proc. Res.*, 9, 240–245 (2008).
20) F. H. Perera, A. Pajares and J. J. Meléndez, *J. Eur. Ceram. Soc.*, 31, 1695–1701 (2011).
21) L. Jiang, X.-Y. Chen, G.-M. Han and Y. Meng, *Trans. Nonferrous Met. Soc. China*, 21, 1574–1579 (2011).
22) Y. Ohya, K. Hamano and Z. Nakagawa, *J. Ceram. Soc. Japan*, 94, 665–670 (1986).
23) Y. Suzuki, T. S. Suzuki, Y. Shinoda and K. Yoshida, *Adv. Eng. Mater.*, 14, 1134–1138 (2012).
24) H. L. Lee, J. Y. Jeong and H. M. Lee, *J. Mater. Sci.*, 32, 5687–5695 (1997).
25) A. Tsetsekou, *J. Eur. Ceram. Soc.*, 25, 335–348 (2005).